Journal of Crystal Growth 435 (2016) 1–5

Contents lists available at ScienceDirect

Journal of Crystal Growth

journal homepage: www.elsevier.com/locate/jcrysgro

Reinvestigation on the phase transition of a LiB_3O_5 crystal near its melting point

S.M. Wan [a,*], G.M. Zheng [a], D.X. Feng [a], Y.N. Yao [a], Y. Zhao [b], J.L. You [c], Z.G. Hu [b,*]

[a] Anhui Key Laboratory for Photonic Devices and Materials, Anhui Institute of Optics and Fine Mechanics, Chinese Academy of Sciences, Hefei 230031, China
[b] Technical Institute of Physics and Chemistry, Chinese Academy of Sciences, Beijing 100190, China
[c] School of Material Science and Engineering, Shanghai University, Shanghai 200072, China

ARTICLE INFO

Article history:
Received 13 October 2015
Received in revised form
5 November 2015
Accepted 6 November 2015
Communicated by: V. Fratello
Available online 24 November 2015

Keywords:
A1. Phase diagrams
A1. Raman spectroscopy
A1. First-principles calculations
B1. Borates
B2. Nonlinear optic materials

ABSTRACT

Raman spectroscopy has been applied to investigate *in-situ* the phase transition of a LBO (LiB_3O_5) crystal near its melting point in order to explain the discrepancies between the experimental results observed in the LBO crystal growth process and the predicted results obtained from the Li_2O–B_2O_3 phase diagram. When the LBO crystal begins to melt, it first decomposes to the kinetic products $Li_2B_4O_7$ and B_2O_3; then the $Li_2B_4O_7$ reacts with the undecomposed LBO to form the thermodynamic product $Li_3B_7O_{12}$. On the basis of these results, a set of models have been proposed to describe the structural transformations present in the phase transition. Additionally, our experimental result indicates that $Li_3B_7O_{12}$ is stable/metastable at room temperature. Its Raman spectrum has been calculated by the density functional theory method for identification of the $Li_3B_7O_{12}$ crystalline phase in a mixture. The result shows that $Li_3B_7O_{12}$ has three strong characteristic Raman peaks located around 595, 775 and 1040 cm^{-1}.

1. Introduction

LBO (LiB_3O_5, lithium triborate) is the most widely used nonlinear optical crystal for generation of the second and third harmonics of 1064 nm radiation from a Nd:YAG laser [1]. In the past two decades, much effort has been devoted to understanding the nucleation and growth of LBO crystals [2]. Some discrepancies between the predicted and experimental results have been found, for example: (1) According to the Li_2O–B_2O_3 phase diagram [3], LBO is the only crystalline phase precipitating out of a B_2O_3 excess LiB_3O_5 high-temperature solution as the temperature decreases. But Markgraf et al. reported that seeding of the solution with a Pt wire sometimes resulted in LTB ($Li_2B_4O_7$, lithium tetraborate) instead of LBO [4]. (2) According to the Li_2O–B_2O_3 phase diagram, LBO first decomposes to $Li_3B_7O_{12}$, which then decomposes to LTB. But Shepelev et al. found that LBO decomposed to LTB or $Li_3B_7O_{12}$ depending on the heating rate [5].

Investigations into the discrepancies can help us to understand the essence of the LBO phase transition deeply and to develop better technique to grow LBO crystals. Structural information is the most important aspect to understand the phase transition but, unfortunately, such information is scarce.

The LBO crystal phase transition occurs above 834 °C, and thus a high-temperature *in-situ* experimental technique is required to gain unambiguous structural information. Raman spectroscopy is a common and effective experimental tool to investigate high-temperature melt/crystal structures. However, due to the complexity of borate melt/crystal structures and their Raman spectra, extraction of the structural information from the Raman spectra is very difficult. Recently, the DFT (density functional theory) method has been successfully applied to establish the links between the structures and spectra of some borate melts/crystals [6–8]. In this paper, Raman spectroscopy combined with the DFT method is employed to obtain structural information on the LBO phase transition in order to understand its essence.

2. Experimental and computational details

The experimental system comprises two parts: a home-made hot stage and a Jobin Yvon LabRaman HR800 Raman spectrometer equipped with a charge-coupled device (CCD) detector. The samples were placed in a platinum boat and heated on the stage. The stage temperatures were measured by a Pt/Rh–Pt thermocouple with an accuracy of about ±1 °C. The Raman spectra were collected with a back-scattering configuration. The 532 nm line of a Q-switched SHG-Nd:YAG laser was used to excite the spectra with an incident power of about 1.0 W. The laser spot on the samples was less than 2 μm in diameter. The spectra were collected in an

* Corresponding authors.
E-mail addresses: smwan@aiofm.ac.cn (S.M. Wan), Hu@mail.ipc.ac.cn (Z.G. Hu).

http://dx.doi.org/10.1016/j.jcrysgro.2015.11.010
0022-0248/

accumulated mode with 100 s integration time. The interesting spectral range is from 100 to 1700 cm^{-1} with a spectral resolution of 2 cm^{-1}.

The $Li_3B_7O_{12}$ Raman spectrum was calculated by the DFT method implemented in CASTEP (Cambridge Sequential Total Energy Package) [9]. The settings were similar to those used for calculating the CsB_3O_5 Raman spectrum. The Wu–Cohen functional of the generalized-gradient approximation (GGA-WC) was employed to represent the exchange–correlation functional in the DFT formalism [10]. Norm-conserving pseudopotentials were applied to describe the electron–ion interactions. The valence electron configurations were $2s^1$ for lithium, $2s^22p^1$ for boron, and $2s^22p^4$ for oxygen. The electronic wavefunction is expanded by using a plane wave basis set with a cut-off energy of 750 eV. The sampling of the Brillouin zone was performed on a $2\times2\times2$ Monkhorst–Pack grid. The SCF (self-consistent field) convergence criterion was set to 1×10^{-6} eV/atom. The calculated Raman intensities were reduced by the Bose–Einstein population factors with the room temperature (300 K) and the excitation source wavelength (The 532 nm line of the Q-switch SHG-Nd:YAG laser).

3. Results and discussion

The CCD detector was employed to monitor the melting process of the LBO crystal. When the crystal began to melt, a crystal coexisted with the melt in the platinum boat (Fig. 1(a)) and we collected the Raman spectra of the crystal (Fig. 2(a)) and the melt (Fig. 2(b)). The crystal spectrum possesses the principal characteristics of LBO [11], indicating that the crystal is LBO and LBO is

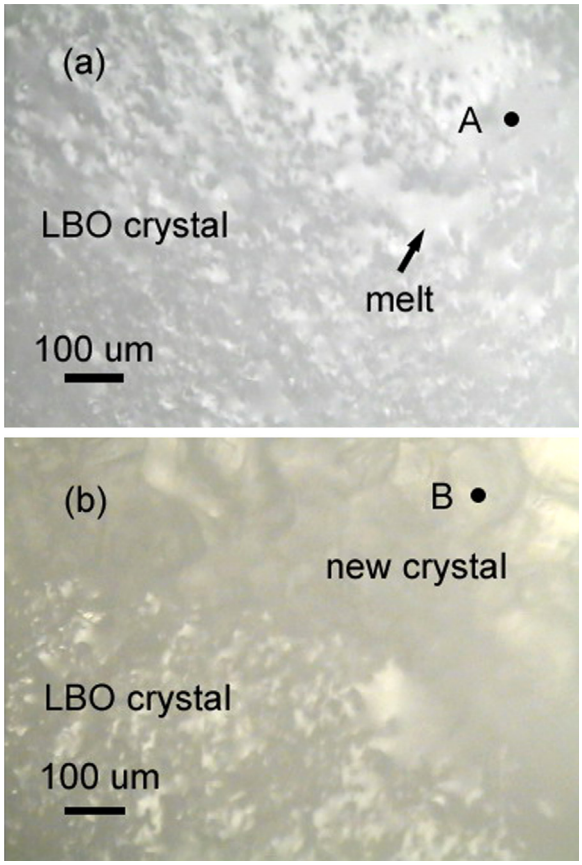

Fig. 1. *In-situ* microphotographs showing the phase transition of the LBO crystal occurring near its melting point. (a) The LBO crystal coexisting with a melt; (b) the LBO crystal coexisting with a new crystal. Positions A and B are in the melt and in the new crystal, respectively.

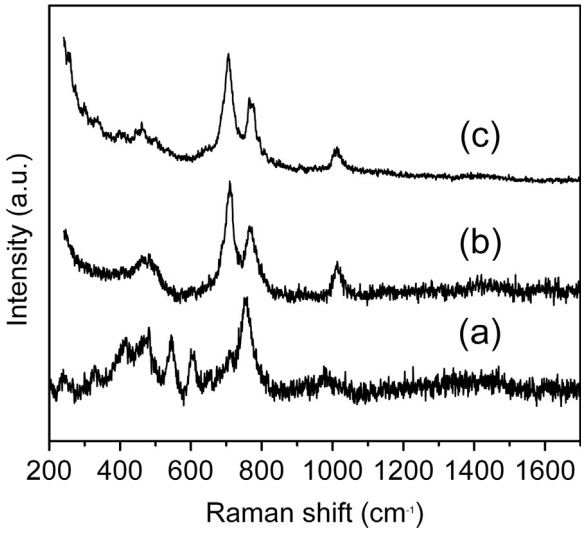

Fig. 2. Raman spectra of (a) the LBO crystal, (b) the melt, and (c) the new crystal growing on the LBO crystal surface.

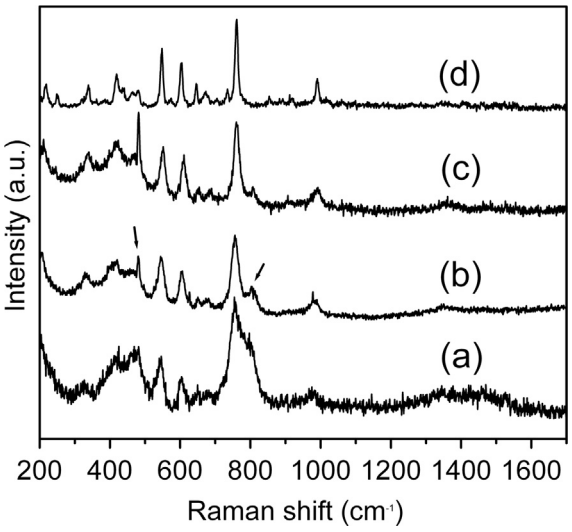

Fig. 3. The Raman spectra recorded on the undecomposed LBO crystal surface at around (a) 840 °C, (b) 600 °C, and (c) 400 °C; (d) the LBO Raman spectrum recorded at room temperature for comparison.

stable below its melting point. The melt spectrum is quite different from the LBO spectrum but very similar to the LTB spectrum [8], showing that the melt has the LTB structural characteristics. Sometimes, a new crystal, which crystallized from the melt, could be observed on the undecomposed LBO crystal surface (Fig. 1(b)). Its Raman spectrum is shown in Fig. 2(c). It is a typical LTB Raman spectrum, indicating the new crystal is LTB. The result further supports that LTB (melt or crystal) is a product of the phase transition.

After the phase transition, we recorded the Raman spectrum on the undecomposed LBO crystal surface (Fig. 3(a)) and found that, besides the LBO characteristic peaks, a shoulder peak located at around 808 cm^{-1} is present at the right side of the strongest peak. The 808 cm^{-1} peak has been assigned to the breathing vibration of the $B_3O_3Ø_3$ ring (Ø=bridging oxygen atom, see Fig. 4), the primary structural group in the B_2O_3 glass/melt [12]. It means that B_2O_3 is another product of the LBO phase transition.

As the temperature decreases, a sharp peak is present at 480 cm^{-1}. Its intensity increases with the decrease of the 808 cm^{-1} peak intensity (see Fig. 3(a)–(c), the two peaks are

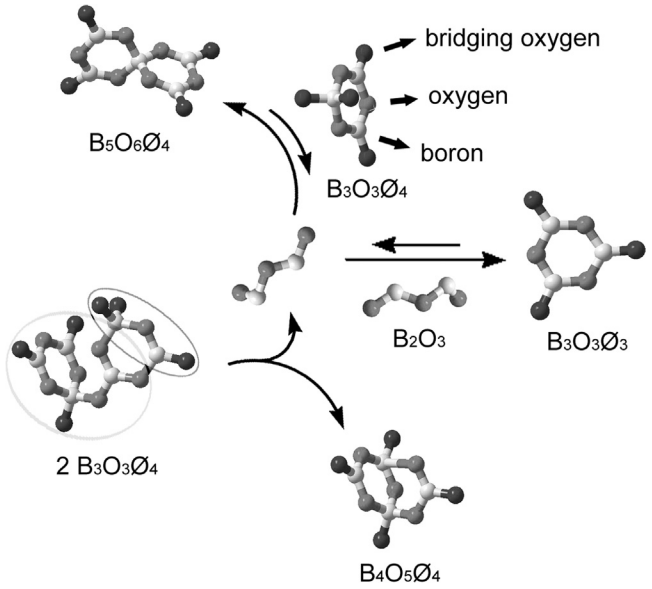

Fig. 4. Structural transformations after the LBO phase transition. $B_3O_3Ø_4$, $B_4O_5Ø_4$, and $B_3O_3Ø_3$ are the basic structural units of the LBO crystal, LTB crystal, and B_2O_3 melt, respectively.

marked by arrows.). The 480 cm^{-1} peak has been assigned to the breathing vibration of a $BØ_4$ unit [13]. It means that the $BØ_4$ content on the LBO surface is negatively correlated to the B_2O_3 content. Considering that $B_5O_6Ø_4$ (see Fig. 4) is the only structural group whose chemical composition is between that of B_3O_5 (LBO) and B_2O_3 [14], we deem that the $B_5O_6Ø_4$ group was formed on the LBO surface by the reaction between LBO and B_2O_3. The well-defined and highly symmetrical $BØ_4$ unit in the $B_5O_6Ø_4$ group gives rise to the 480 cm^{-1} sharp peak.

On the basis of the above analyses, a set of structural models are proposed for better describing and understanding the LBO phase transition (Fig. 4). When the LBO crystal melts, two $B_3O_3Ø_4$ rings (the basic structural group of LBO [15]) transform to a $B_4O_5Ø_4$ group (the basic structural group of LTB [16]) and a B_2O_3 molecule. The B_2O_3 molecules further polymerize to $B_3O_3Ø_3$ rings (the basic structural group of the B_2O_3 melt), or react with the undecomposed $B_3O_3Ø_4$ rings to form the $B_5O_6Ø_4$ groups.

The Li_2O–B_2O_3 phase diagram shows that LBO is the only phase crystallizing from a B_2O_3 excess LiB_3O_5 high-temperature solution as the temperature decreases. However, Markgraf et al. found that seeding of the solution with a platinum wire sometimes resulted in LTB instead of LBO [4]. We deem that the disagreement between the phase diagram and the experimental result originates from the LBO phase transition mentioned above and is related to the high viscosity of the solution [17]. The raw material for the LBO crystal growth is a mixture of LBO and B_2O_3. As the raw material is heated above the LBO phase transition temperature, the LBO will decompose to LTB melt/crystal. But the LTB melt/crystal is hard to react with other solution components to form LBO building units because the mass transport is very difficult in a solution of high viscosity. As a result, LTB tends to crystallize out from the solution rather than LBO. In order to avoid the formation of LTB, the high-temperature solution should be fully stirred or be held at a sufficiently high temperature for a sufficiently long time to ensure that the LTB has been transformed to the LBO building unit.

According to the Li_2O–B_2O_3 phase diagram, LBO first decomposes to $Li_3B_7O_{12}$ (834 °C), which then decomposes to LTB (875 °C), but the predicted results are in conflict with our experimental results. Our results show that LBO first decomposes to LTB instead of $Li_3B_7O_{12}$. Additionally, Kaplun et al. observed that LBO melted incongruently in two ways and decomposed to either LTB or

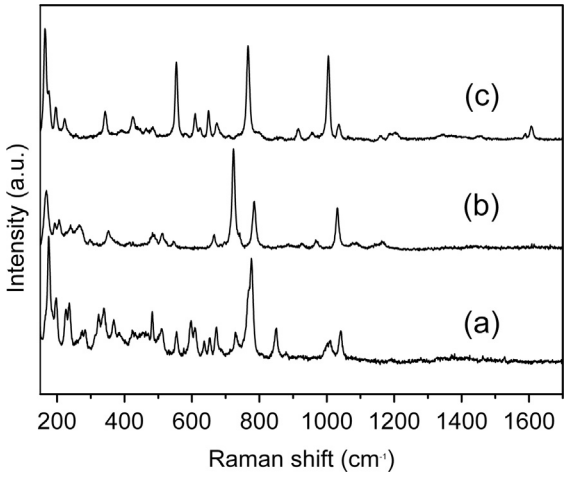

Fig. 5. The Raman spectrum of (a) a polycrystalline product obtained by cooling; the Raman spectra of (b) LBO and (c) LTB for comparison.

$Li_3B_7O_{12}$ [18,19]. Shepelev et al. considered that LBO decomposes to LTB or $Li_3B_7O_{12}$ depending on the heating rate [5]; however, this assumption needs further supporting evidence.

As we know, a phase diagram only represents the phase relationships under equilibrium conditions, but LBO decomposition is probably a non-equilibrium process. Therefore, we think that LTB is likely the kinetic product of LBO decomposition and $Li_3B_7O_{12}$ is the thermodynamic product. In order to prove the conjecture, a LBO crystal slice was heated in a platinum boat to about 845 °C (part of the crystal will decompose at this temperature) and held at the temperature for about 1 h. After that, the sample was cooled to room temperature at a rate of about 5 °C/min. A white polycrystalline mixture was formed in the platinum boat. Raman spectra from different parts of the polycrystalline mixture were collected. The results show that different positions have different Raman spectra (see the Supporting information Fig. S1 for more details.). It is noteworthy that, except for the characteristic peaks of LBO and LTB, a set of new Raman peaks are present. A typical spectrum including these peaks is shown in Fig. 5(a).

The new Raman peaks are most likely to be associated with $Li_3B_7O_{12}$. However, the $Li_3B_7O_{12}$ Raman spectrum has not been reported. In 1990, Jiang et al. obtained a $Li_3B_7O_{12}$ crystal by the flux method and determined its crystal structure [20]. On the basis of the crystal structure, we calculated its Raman spectrum by the DFT method, which has been successfully applied to calculate the Raman spectra of other borate crystals such as CsB_3O_5, BiB_3O_6 and LTB [6–8]. Fig. 6 shows the calculated spectrum of $Li_3B_7O_{12}$, which has three strong characteristic peaks located around 595, 775 and 1040 cm^{-1} (see the Supporting information Table S1 for more details.). Except for a small number of Raman peaks, for example the 480 cm^{-1} peak, which are probably attributed to other products, most of the experimental peaks are consistent to the calculated peaks in frequency and intensity. The consistency confirms that these new Raman peaks arise from $Li_3B_7O_{12}$ and thus proves that $Li_3B_7O_{12}$ is a product of the heat treatment. The above results demonstrate that $Li_3B_7O_{12}$ can be produced by prolonging the reaction time after the LBO phase transition. Therefore, $Li_3B_7O_{12}$ is the thermodynamic product of the LBO phase transition.

By studying the compositions and the structures of LTB, $Li_3B_7O_{12}$, and LBO, we consider that $Li_3B_7O_{12}$ is the product of the reaction between the intermediate product LTB and the undecomposed LBO. In a previous paper, we have studied the structural transformation of the $B_4O_5Ø_4$ group (the basic structural group of LTB) and found that the $B_4O_5Ø_4$ group can transform to the $B_4O_6Ø_2$ group (see Fig. 7) at high temperatures [8]. In the same way, the

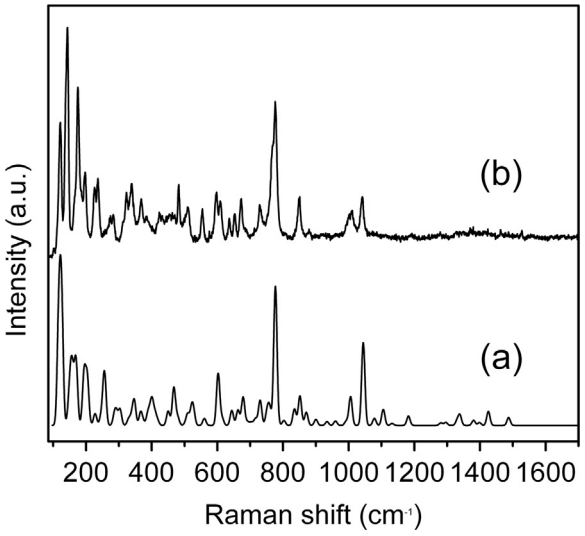

Fig. 6. (a) The calculated Raman spectrum of $Li_3B_7O_{12}$, and (b) the experimental Raman spectrum of a polycrystalline compound in the platinum boat.

$B_4O_5Ø_4$ group produced by the LBO decomposition will change to the $B_4O_6Ø_2$ group, which then connects with the $B_3O_3Ø_4$ group (the basic structural group of LBO) to form the $B_7O_9Ø_6$ group, the basic structural group of $Li_3B_7O_{12}$ [20], as shown in Fig. 7.

According to the Li_2O–B_2O_3 phase diagram, $Li_3B_7O_{12}$ is stable in the temperature range of 696–856 °C. However, our experimental result shows that $Li_3B_7O_{12}$ is stable/metastable at room temperature, which is inconsistent with the phase diagram, but is consistent with the reported results. For example: (1) Jiang et al. obtained a $Li_3B_7O_{12}$ single crystal by the flux method and found the crystal to be stable at room temperature [20]. (2) Shinsho et al. synthesized Cu:$Li_3B_7O_{12}$ polycrystalline powder by the method of solid-state reaction, and studied its basic thermo-luminescence characteristics at temperatures below 180 °C [21].

4. Conclusions

The phase transition of the LBO crystal near its melting point has been investigated by *in-situ* Raman spectroscopy with the help of the DFT method in order to explain the discrepancies between the experimental results observed in the LBO crystal growth process and the predicted results obtained by the Li_2O–B_2O_3 phase diagram. When the crystal melts, it first decomposes to the kinetic products, LTB melt/crystal and B_2O_3 melt; then, the B_2O_3 melt reacts with the undecomposed LBO to form the $B_5O_6Ø_4$ group. By prolonging the reaction time, the LTB melt/crystal further reacts with the undecomposed LBO to form the thermodynamic product $Li_3B_7O_{12}$. Our result shows that $Li_3B_7O_{12}$ is stable/metastable at room temperature. Its Raman spectrum has been calculated. The result shows that $Li_3B_7O_{12}$ has three strong characteristic Raman peaks located around 595, 775 and 1040 cm^{-1}.

The structural details of the LBO phase transition have been provided. When LBO melts, two $B_3O_3Ø_4$ rings (the basic structural unit of LBO) transform to a $B_4O_5Ø_4$ group (the basic structural group of LTB) and a B_2O_3 molecule. The B_2O_3 molecules further polymerize to the $B_3O_3Ø_3$ rings (the basic structural group of the B_2O_3 melt), or react with the $B_3O_3Ø_4$ rings to form $B_5O_6Ø_4$ groups. With an increase of the heat treatment time, the $B_4O_5Ø_4$ groups gradually change to $B_4O_6Ø_2$ groups which then react with the $B_3O_3Ø_4$ rings to form $B_7O_9Ø_6$ groups (the basic structural groups of $Li_3B_7O_{12}$).

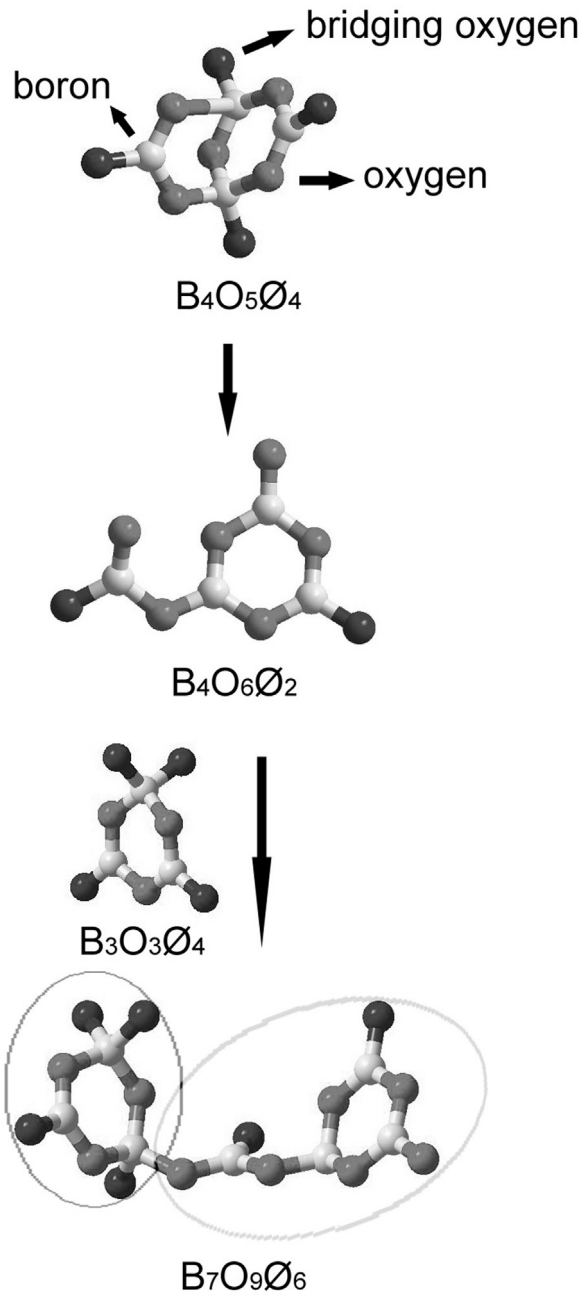

Fig. 7. The structural transformation from $B_4O_5Ø_4$ (the basic structural group of LTB) to $B_7O_9Ø_6$ (the basic structural group of $Li_3B_7O_{12}$).

Acknowledgment

This work is financially supported by the National Natural Science Foundation of China (Grant nos. 51372246 and 51132005).

Appendix A. Supplementary material

Supplementary data associated with this article can be found in the online version at http://dx.doi.org/10.1016/j.jcrysgro.2015.11.010.

References

[1] D.N. Nikogosyan, Lithium triborate (LBO): a review of its properties and applications, Appl. Phys. A 58 (1994) 181–190.

[2] S.M. Wan, The growth of borate nonlinear optical crystals, in: G.V. Karas (Ed.), New Developments in Crystal Growth Research, Nova Science Publishers, Virgina, 2006, pp. 1–38.
[3] B.S.R. Sastry, F.A. Hummel, Studies in lithium oxide systems: I, $Li_2O \cdot B_2O_3 - B_2O_3$, J. Am. Ceram. Soc. 41 (1958) 7–17.
[4] S.A. Markgraf, Y. Furukawa, M. Sato, Top-seeded solution growth of LiB_3O_5, J. Cryst. Growth 140 (1994) 343–348.
[5] F. Yu., R.S. Shepelev, S.K. Bubnova, N.A. Filatov, N.A. Sennova, Pilneva, LiB_3O_5 crystal structure at 20, 227 and 377 °C, J. Solid State Chem. 178 (2005) 2987–2997.
[6] M. Hou, J.L. You, S. Patrick, G.C. Zhang, S.M. Wan, Y.Y. Wang, Z.F. Ji, L.H. Wang, P. Z. Fu, Y.C. Wu, S.T. Yin, High temperature Raman spectroscopic study of the micro-structure of a caesium triborate crystal and its liquid, CrystEngComm 13 (2011) 3030–3034.
[7] Y.L. Sun, S.M. Wan, X.S. Lv, X.L. Tang, J.L. You, S.T. Yin, New insights into the BiB_3O_6 melt structure, CrystEngComm 15 (2013) 995–1000.
[8] S.M. Wan, X.L. Tang, Y.L. Sun, G.C. Zhang, J.L. You, P.Z. Fu, Raman spectroscopy and density functional theory analyses on the melt structure in the $Li_2B_4O_7$ crystal growth system, CrystEngComm 16 (2014) 3086–3090.
[9] V. Milman, K. Refson, S.J. Clark, C.J. Pickard, J.R. Yates, S.P. Gao, P.J. Hasnip, M.I. J. Probert, A. Perlov, M.D. Segall, Electron and vibrational spectroscopies using DFT, plane waves and pseudopotentials: CASTEP implementation, J. Mol. Struct.: THEOCHEM 954 (2010) 22–35.
[10] Z. Wu, R.E. Cohen, More accurate generalized gradient approximation for solids, Phys. Rev. B 73 (2006) 235116.
[11] Y.J. Jiang, Y. Wang, L.Z. Zeng, Analysis of Raman spectra of LiB_3O_5 single crystals, J. Raman Spectrosc. 27 (1996) 601–607.
[12] G.E. Walrafen, S.R. Samanta, P.N. Krishnan, Raman investigation of vitreous and molten boric oxide, J. Chem. Phys. 72 (1980) 113–120.
[13] E.I. Kamitsos, M.A. Karakassides, Structural studies of binary and pseudo binary sodium borate glasses of high sodium content, Phys. Chem. Glas. 30 (1989) 19–26.
[14] E.I. Kamitsos, G.D. Chryssikos, Borate glass structure by Raman and infrared spectroscopies, J. Mol. Struct. 247 (1991) 1–16.
[15] N. Sennova, R. Bubnova, J. Shepelev, S. Filatov, O. Yakovleva, $Li_2B_4O_7$ crystal structure in anharmonic approximation at 20, 200, 400 and 500 °C, J. Alloy. Compd. 428 (2007) 290–296.
[16] H. Konig, R. Hoppe, Borates of alkaline-metals. 2, Knowledge of LiB_3O_5, Z. Anorg. Allg. Chem. 439 (1978) 71–79.
[17] H.B. Liu, G.Q. Shen, X.Q. Wang, J.Z. Wei, D.Z. Shen, Viscosity and IR investigations in the $Li_2O-B_2O_3$ system, Prog. Cryst. Growth Charact. 40 (2000) 235–241.
[18] A.B. Kaplun, A.B. Meshalkin, Phase equilibria in the Li_2O–B_2O_3 system, Inorg. Mater. 35 (1999) 1154–1158.
[19] A.B. Kaplun, A.B. Meshalkin, Phase equilibria in the binary systems Li_2O–B_2O_3 and Cs_2O–B_2O_3, J. Cryst. Growth 209 (2000) 890–894.
[20] A.D. Jiang, S.R. Lei, Q.Z. Huang, T.B. Chen, D.M. Ke, Structure of lithium heptaborate, $Li_3B_7O_{12}$, Acta Crystallogr. Sect. C: Cryst. Struct. Commun. 46 (1990) 1999–2001.
[21] K. Shinsho, Y. Koba, G. Wakabayashi, S. Tamatsu, S. Fukuda, R. Morimoto, D. Maruyama, H. Saitoh, N. Sakurai, Basic characteristics of tissue-equivalent phantom thermoluminescence slab dosimeter using new TL phosphor $Li_3B_7O_{12}$:Cu, Radiat. Meas. 62 (2014) 15–21.